Journal of Fluids and Structures (1999) **13,** 755–778
Article No.: jfls.1999.0226 available online at http://www.idealibrary.com on IDEAL

AERODYNAMICALLY GENERATED ACOUSTIC RESONANCE IN A PIPE WITH ANNULAR FLOW RESTRICTORS

A. K. Stubos*, C. Benocci, E. Palli, G. K. Stoubos, and D. Olivari

Von Karman Institute for Fluid Dynamics
1640 Rhode-St-Genese, Belgium

(Received 11 April 1997 and in finally revised form 29 January 1999)

An experimental study of the coupling between fluid dynamic instabilities and an acoustic field is performed for the case of a pipe with annular flow restrictors, representing a segmented solid propellant booster. As long as the distance between the restrictors remains smaller than the length of the flow recovery region behind the upstream restrictor, the fluid flow can amplify the acoustic pereturbations at the frequencies of the acoustic modes, leading to strong resonance for specific flow velocity ranges. A physical explanation is proposed, linking the amplification of the acoustic perturbation to the phase and frequency of vortex shedding from the restrictors. An approximate semi-empirical correlation is developed for the critical Strouhal number of the phenomenon as a function of the restrictor size and other problem parameters.

1. INTRODUCTION

Flow induced acoustic resonance in piping systems has been recently investigated with application to self-sustained aero-acoustic pulsations in gas transport systems (Bruggeman *et al.* 1991; Kriesels *et al.* 1995). Earlier work has provided insight to the related basic fluid mechanical aspects of shear flow instability and transition to turbulence (Tritton 1988) and self-sustaining oscillations of flow past cavities (Rockwell & Naudascher 1978). The same phenomenon has been found in the past to lead to uncontrolled burning rates and vibrations inside the combustion chamber of solid-propellant rocket motors (Brown *et al.* 1981; Hegde & Strahle 1985). More specifically, the presence of important flow restrictions, due to flange-type structures between different solid fuel grain segments, causes the formation of shear layers, which can eventually interact to produce a self-sustained oscillating system. Flandro (1986) used linear stability theory to investigate the coupling of acoustic and vortical oscillations in a rocket combustion chamber. The results suggest that a feedback loop may exist between sound field and shear layer growth.

More recently, Huang & Weaver (1991) have shown multiple coherent vortices over a cavity between annular restrictors and discussed the mechanics of pipeline resonance and active control of shear-layer instability. Coherent vortex structures are reported to develop on a free shear layer causing acoustic resonance upon impingement on a downstream surface. Hourigan *et al.* (1990) have studied the acoustic response of a rectangular duct containing a pair of fixed restrictions in terms of the flow characteristics and the acoustic field near the restrictors. On the basis of theoretical arguments and experimental data, the

* Present address: NCSR Demokritos, 15310 Ag. Paraskevi Attikis, Greece.

0889–9746/99/060755 +24 $30.00

conclusion is reached that a feedback loop can be established under certain conditions between the sound field and vortex shedding from the restrictors. This phenomenon can be observed for several flow velocity ranges, the common factor being the phase relationship between the vortex reaching the downstream restrictor and the resonant acoustic cycle. For certain flow velocity ranges, the phase relationship is such that sufficient positive net acoustic energy is produced to sustain resonance and the feedback loop. Similar synchronization of vortex shedding with a natural acoustic frequency in rectangular ducts has also been observed experimentally by Nomoto & Culick (1982) although acoustic feedback was not identified as the responsible mechanism by these authors.

The present work aims at confirming and extending the conclusions of Hourigan *et al.* (1990) through an investigation of the effect of different parameters on the flow-acoustic coupling and the resulting resonance in a cylindrical tube containing one or two annular flow restrictors. In particular, the influence of distance between restrictors, their size and geometrical shape as well as of the flow velocity was studied in the present test program, to obtain an improved understanding of fluid-dynamic–acoustic interactions in rocket boosters. The mechanism proposed by Hourigan *et al.* (1990) is extended by deriving an approximate predictive correlation incorporating the effect of geometrical and flow parameters. The differences between the present results and other related experimental data reported in the literature are discussed and physical explanations are presented. Other issues relevant to the case of a rocket combustion chamber such as the role of side-flow injection and the possibility of eliminating resonance are also examined. It is important to notice though that the present study focuses on the phenomenology observed in the case of a set-up characterized by axial flow only. Significant effects of side flow, sonic conditions at the outlet of the tube and outlet nozzle shape are examined in detail elsewhere (Anthoine *et al.* 1998a, b).

2. EXPERIMENTAL SET-UP AND PROCEDURE

The test-section has been designed to reproduce the geometry of a typical solid-fuel rocket motor as the one sketched in Figure 1, consisting of a hemispherical head, two quasi-cylindrical fuel grains separated by restrictors, and a contoured nozzle. By restricting the investigation to times larger than $T/4$, where T is the total combustion time, the head can be assumed inactive and replaced by an aerodynamically shaped inlet; the resulting model is shown in Figure 2: besides the inlet, it is composed of two cylindrical elements of length around 0·6 m and diameter $D = 0{\cdot}15$ m and a nozzle of diameter $d_n = 0{\cdot}059$ m; restrictors with square edges of thickness 1–2 mm and different internal diameters can be inserted between the segments.

Each of the cylindrical segments possesses a longitudinal array of 12 access holes for instrumentation as well as two circumferential arrays of six access holes each, as shown in

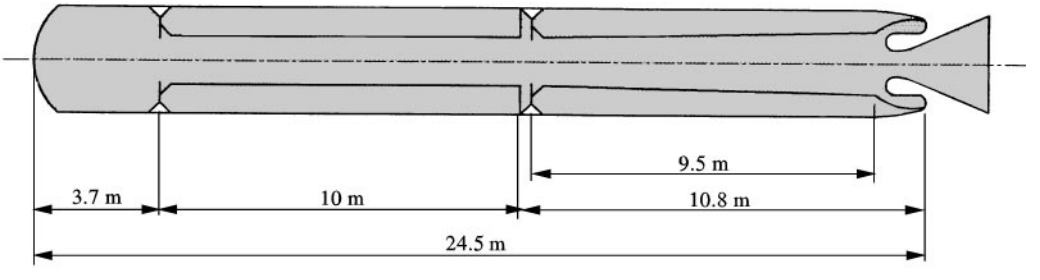

Figure 1. Schematic of rocket motor.

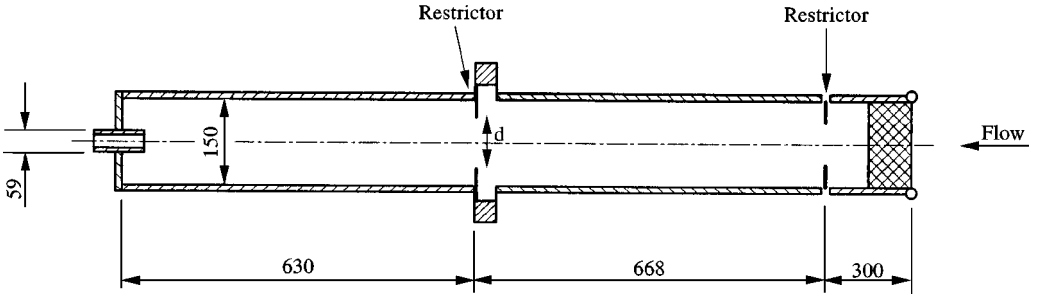

Figure 2. Schematic of the test-section (dimensions in mm).

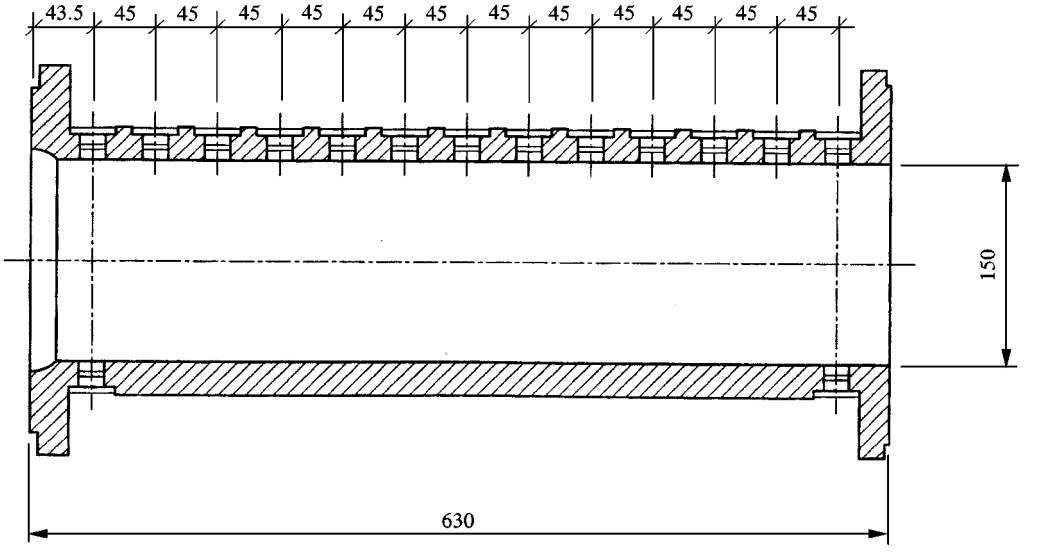

Figure 3. Cylindrical segment with instrumentation holes (dimensions in mm).

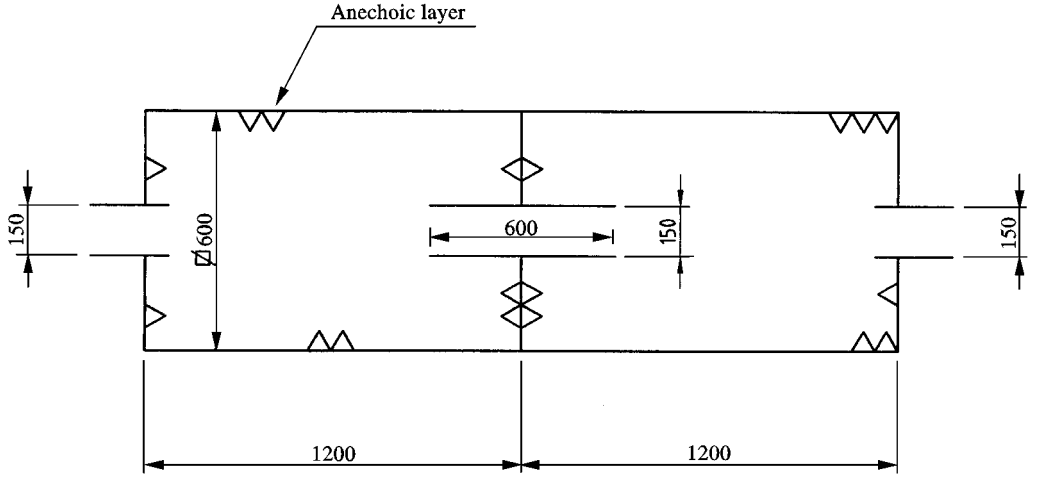

Figure 4. Sound muffler (dimensions in mm).

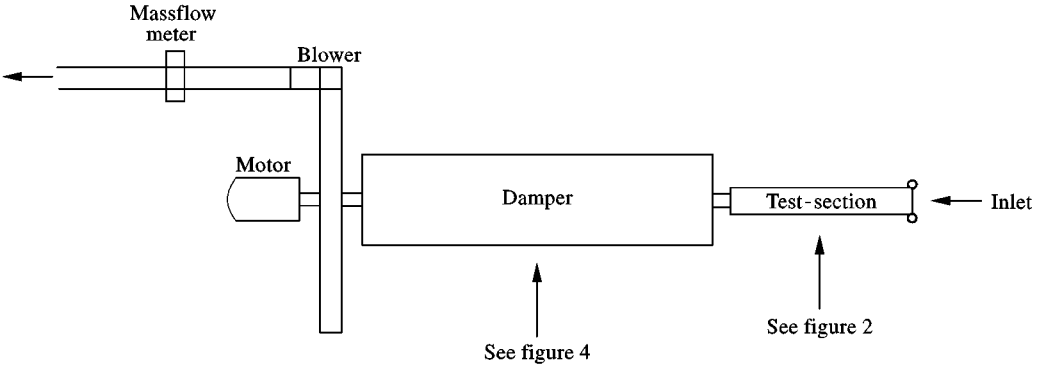

Figure 5. Sketch of experimental apparatus.

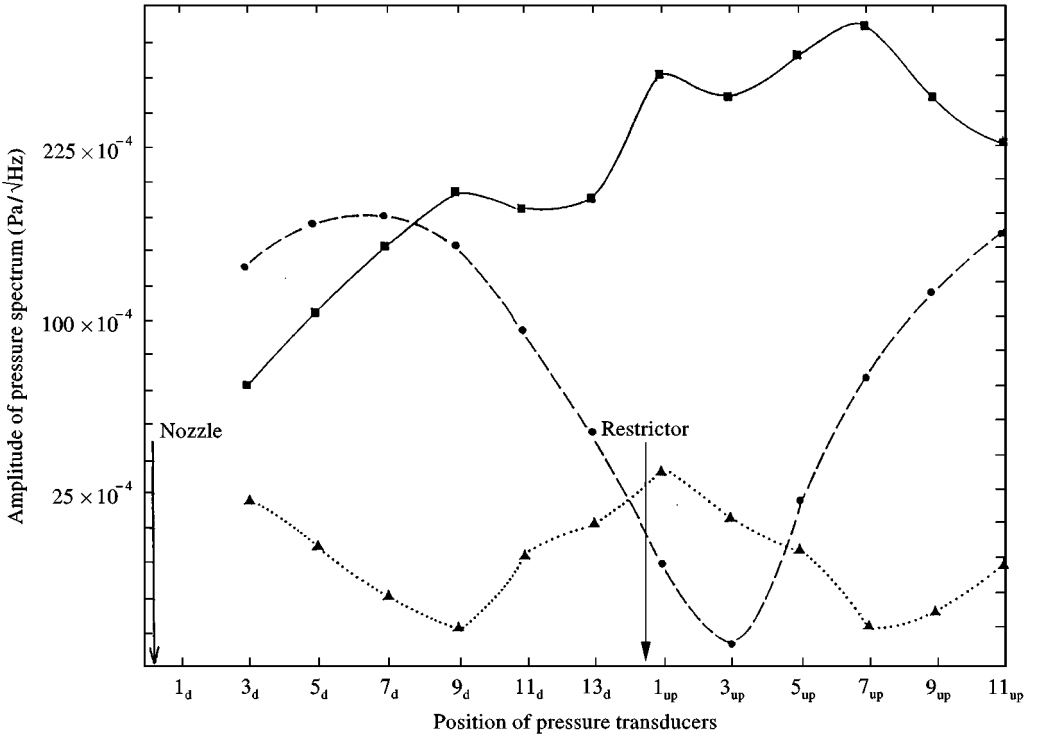

Figure 6. Shape of typical acoustic modes in the tube (the different symbols correspond to different acoustic modes).

Figure 3, in order to allow for the investigation of both axial and circumferential instability modes.

Instrumentation includes hot-wire anemometers (HW, Series 7 made by VKI) mounted on probe-traversing mechanisms (from the wall to the cylindical axis) for velocity measurements, and piezoelectric transducers Mod 106B50 from PCB Piezotronics Inc. for pressure fluctuation measurements on the pipe wall. Hot-wire data were linearized and acquisition was made using a 16-channel DAS 20 card on PC. Data processing is based upon a HP-35660A two-channel spectrum analyser.

The working fluid is air, driven by a blower installed downstream of the nozzle, which allows for mean flow velocity values between 8 and 40 m/s (Re = 80 000 to 400 000 for a Reynolds number based upon the test-section diameter and mean flow velocity). To avoid any influence of the blower on the acoustic behaviour of the test-section, a muffler is interposed between the two. It consists of two boxes of square cross-section (1·2 m long and 0·6 m wide each) connected via a pipe of 0·6 m length and 0·15 m diameter (Figure 4). The internal walls of the boxes are covered by an anechoic material to enhance their performance. Good damping was found over the whole range of frequencies of interest (50–400 Hz). For the range of flow velocities tested, no significant interference from the muffler (e.g. inlet pulsation) was detected. Preliminary experiments with and without the muffler did not result in any appreciable variation in the pipe resonant frequencies. A full sketch of the facility can be seen in Figure 5.

The shape and frequency of the acoustic modes of the test-section were determined in the absence of flow, subjecting it to a sinusoidal acoustic signal of constant power and varying frequency or to a random signal. A loudspeaker, driven by a signal generator, was used for this purpose. The amplitude of the response has been recorded by the pressure transducers and was found to be the same for both the sinusoidal and the random signals. For a typical configuration of two restrictors of 0·125 m internal diameter spaced by 0·6 m, the acoustic mode frequencies were found to be 68, 157, 223, 277 Hz for the 1st, 2nd, 3rd and 4th harmonics, respectively. Very slight variation of these values is found as the internal diameter and/or the distance between the restrictors are changed. The acoustic source was removed when air flow was initiated in the test-section and the resonant frequencies were very close to those found in the absence of flow. The measured frequencies are reasonably well approximated by the formula (pressure node at the open boundary):

$$\mathrm{f}_i = i\,\frac{c}{4L}, \quad i = 1, 2, \ldots,$$

where L is the length of the test-section. The shape of typical acoustic standing waves along the test-section is shown in Figure 6. Any irregularities should be attributed to the geometric features (cavity, restrictors) of the pipe interior and the presence of the nozzle (which gives the respective boundary a hybrid character). Note that the open boundary lies a certain distance to the right of the position 11_{up} in Figure 6.

The restrictor located at $L/2$ is very close to a pressure node for the second mode (around position 3_{up} in Figure 6), and can therefore be expected to favour the excitation of that harmonic (Dunlap & Brown 1981; Flatau & Van Moorhem 1990).

In spite of the well-known sensitivity of acoustic phenomena to all possible sources of external perturbation, an acceptable level of repeatability was achieved. The maximum scatter between different experiments under similar conditions was less than 10% for the energy associated with the resonant acoustic peak and 8% for the corresponding value of flow velocity.

3. EXPERIMENTAL RESULTS

3.1 Preliminary Observations

A series of preliminary tests have been run where the flow velocity in the tube was gradually increased from zero to its maximum value. These experiments have established that no purely fluid dynamic vortex shedding, in the form of repeatable and predictable vortex rings characterized by a constant Strouhal number, can be sustained in the present geometry, except for some very narrow ranges of flow conditions. In practical terms, no phenomenon

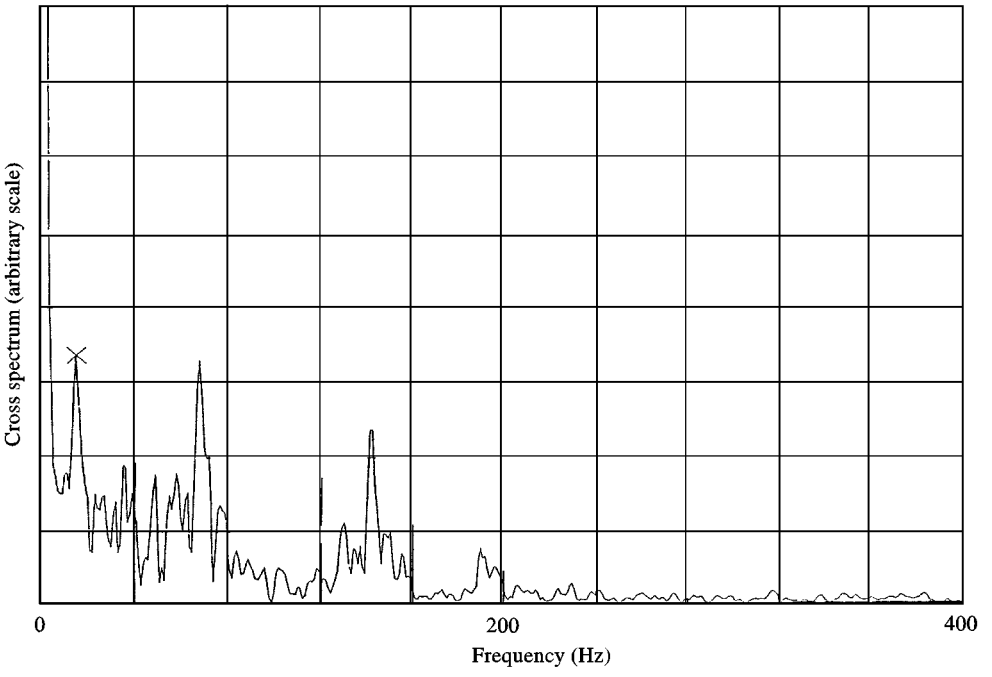

Figure 7. Cross-spectrum of hotwire and pressure transducer signals for $U = 24$ m/s.

characterized by a frequency changing linearly with flow velocity can be observed in either the pressure or the velocity signals (a few exceptions will be commented upon later on). On the contrary, as shown by the typical cross-spectrum between the signal from the hot wire and the one from the nearest pressure transducer in Figure 7, significant unsteadiness exists for the whole range of flow velocities investigated, at frequencies close to the first two acoustic modes of the system (69 and 144 Hz). The strength of the phenomenon was found to depend on the spacing between restrictors.

This result is in disagreement with the widely held view (Brown *et al.* 1981) that the presence of restrictors in the segmented booster gives rise to well-organized vortex shedding for all flow velocities satisfying Reynolds similarity (i.e., developed turbulent flow). In the present configuration, it is found that any perturbation due to geometrical irregularities within the flow field quickly decays to broadband turbulence, except if "organized" by a superimposed acoustic field. In this case, a sustained instability can be found for some flow velocity ranges, and the frequencies of both vortex shedding and sound field coincide with an acoustic mode. The phenomenon is therefore mainly a function of the system geometry. Similar observations were made in a tube with a pair of annular flow constrictions by Dunlap & Brown (1981). It can be concluded that the influence of the acoustic field on the development of flow instabilities is important and the mechanism controlling the interaction and leading to resonance for specific flow velocities must be fundamentally different from the one for the case of jet–edge interactions, which has been proposed as a possible explanation for the fluid dynamic-acoustic coupling in solid-fuel rocket motors. Indeed, in this last phenomenon, the self-sustained oscillations observed arise from purely hydrodynamic perturbations and there is no sound amplification by reflections. In addition, the frequencies of the oscillations and the accompanying sound level are dependent on the

flow velocity, in contrast to the behaviour of the present system.[1] On the basis of the aforementioned preliminary tests, it becomes evident that the Strouhal number to be used in any attempt to quantify the phenomenon should be defined as

$$S = \frac{f_i l}{\overline{U}}, \tag{1}$$

where f_i is the frequency of the ith acoustic mode, U the mean flow velocity in the tube, and l the distance between the restrictors. In the following, f_i will be taken equal to the frequency $f_2 = 158$ Hz of the 2nd harmonic, corresponding to a wavelength approximately equal to $2L$, because this mode was found to be the dominant and most easily excited one in almost all tests performed. This behaviour is due to the existence of a pressure node for this harmonic very close to the location ($L/2$) of the downstream restrictor.

3.2 The Case Of A Single Restrictor

The actual physical mechanism producing fluid-dynamic-acoustic coupling in the case of a single restriction within the flowfield has not yet been clearly identified, and different hypotheses have been proposed. A vortex generated by any source upstream of the restrictor will produce positive or negative acoustic energy, depending on the phase of the acoustic cycle at the moment of vortex passage past the restrictor (Hourigan *et al.* 1990). In the present geometry, no appreciable source of flow instabilities exists between inlet and restrictor; it is instead possible for vortices generated by the restrictor itself to impinge on the nozzle and give rise to acoustic disturbances, which in turn propagate upstream and can be locally amplified by the diffraction around the restrictor edge. As a result, the shear layer near the separation point is perturbed, and this perturbation propagates downstream, making the whole process self-sustaining. This coupling between vortical and acoustic disturbances, however, has been found to lead to velocity-dependent frequencies of oscillation (Jou & Menon 1990), in disagreement with the present findings, as previously discussed. Another mechanism that may lead to pressure fluctuations in the tube can be proposed, assuming the vortices to behave as sources independent of the acoustic modes: when the space–time distribution of these sources contains one of the acoustic modes of the system, resonant oscillations may result. Numerical simulations of cold flows in an axisymmetric ramjet combustor (Menon & Jou 1990), where the instabilities created by a backward-facing step impinge on a downstream choked nozzle, show the presence of both mechanisms and indicate that the second one causes oscillations (at an acoustic frequency) of considerably larger amplitude than the first one, at least for the geometry studied.

In the present test program, the flow phenomenology due to the existence of a *single* restrictor is studied for the case of an obstacle at the position $L/2$; it has to be noted (Figure 2) that the restrictor is installed downstream of an enlargement (cavity), reproducing the end-side surface of a fuel grain.

In this specific configuration, rather moderate pressure oscillations are detected at the frequencies of the first two acoustic modes (70 and 158 Hz). The excitation of the second mode is generally more pronounced, especially for certain velocity values in the tube. The energy content of the pressure signal (amplitude of pressure spectrum) associated with this frequency is shown in Figure 8 as a function of the mean flow velocity for three restrictor sizes (internal diameters of $d_1 = 0{\cdot}115$ m, $d_2 = 0{\cdot}125$ m and $d_3 = 0{\cdot}134$ m); the general trend

[1] On this issue one of the anonymous referees suggested that theoretical results contradict the point made here. Presently, the authors are unable to provide an explanation for this apparent discrepancy.

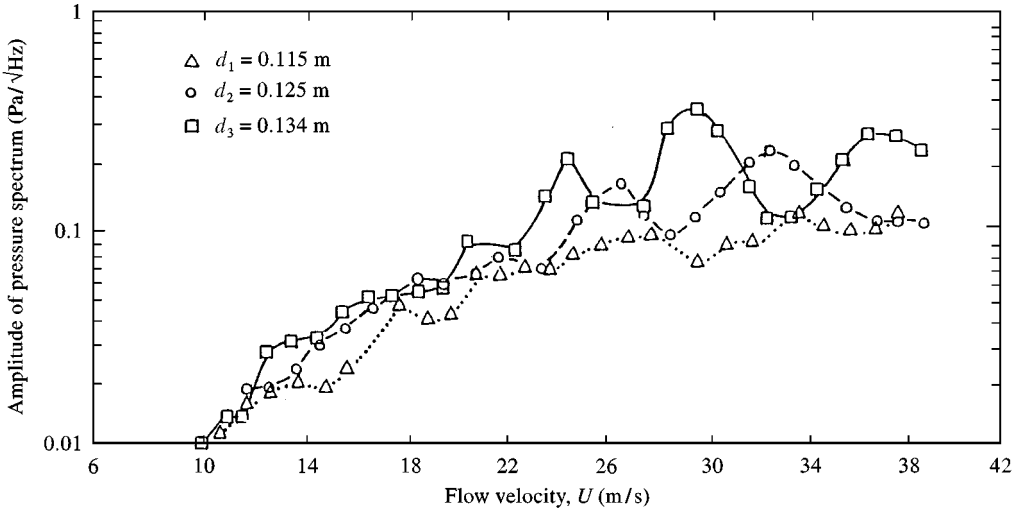

Figure 8. Amplitude of pressure spectrum at f_2 versus mean velocity for the single restrictor case.

is a linear increase of the pressure spectral density (energy content) with flow velocity, but slightly higher values, which are interpreted as weak resonances, can be observed for some specific velocity ranges for d_2 and d_3; on the contrary, no such behaviour is visible for d_1. This trend is consistent with the results of Michalke (1972), which show that thinner shear layers are related to larger growth rates of vortical disturbances, but it is also likely to be influenced by the presence of the small cavity just upstream of the obstacle (Figure 2) which promotes the development of turbulence. In fact, hot wire measurements taken 0·010 m upstream of the restrictor, show the region of highest turbulence to lie very close to the cavity edge. Therefore, the lower the obstruction, the higher will be the turbulence level of the flow impinging on it, which will promote the generation of vortical disturbances that may interact with the downstream nozzle. The specific flow conditions which seem to favour instability for the present case will be discussed in detail in the next section, together with the case of a restrictor pair. For now, it can be concluded that in the present configuration, characterized by relatively high d/D values (in the range of 0·7–0·9) as well as by rather high (of the order of 50–60) ratios of the restrictor–nozzle distance to the restrictor height, the interaction between obstruction and nozzle is generally weak and does not lead to significant levels of self-sustained resonance.

3.3. The Case Of A Restrictor Pair

When two restrictors are present, the main difference with respect to the case previously discussed lies in the possible existence of important interaction between restrictors, which can lead to sustained resonance, locked-on to the frequency of the acoustic mode and characterized by a high-energy content. As will be shown, for a given restrictor size, the possibility of strong mutual interaction is related to the distance l separating the obstacles.

Following Hourigan *et al.* (1990), it is expected that the generation of self-sustained acoustic resonance in the tube will depend on the phase of the acoustic oscillation at which a vortex shed by the upstream restrictor passes the downstream one. This phase is obviously determined by the time needed for the vortex to travel the distance between the obstacles and, therefore, it should be a function of l and the convection speed of flow disturbances. While the study of Hourigan *et al.* refers to a single l value, in the present investigation

a parametric study of the influence of l upon the fluid dynamic-acoustic interaction is undertaken keeping fixed the restrictor at $L/2$ and installing a second restrictor in the test-section at variable distances from the first. During preliminary tests, it was found that the results depend only on l and not on whether the moving restrictor is placed upstream or downstream of the fixed one: the parametric study described in the present section has been performed with the moving restrictor always in the *upstream* position.

The evolution of the energy level associated with the second acoustic mode for the three restrictors is presented in Figures 9–11 for the domain (l-values) over which strong interaction is present [Figures 9(a), 10(a), 11(a)] and for those distances where the response is of the same order as for the single restrictor case [Figures 9(b), 10(b), 11(b)].

Figure 9(a) shows that, for the restrictor d_1, resonant behaviour exists for two different velocity ranges, for l values up to almost 0·3 m. It is also observed that, for a fixed l, the velocity values at which the highest levels of energy are found are separated by a factor of roughly two. The pass-band and the energy level of the first resonant range are almost twice as large as those of the second range. Moving to $l > 0{\cdot}3$ m [Figure 9(b)] the energy level decreases by almost one order of magnitude and the two peaks become gradually less and less distinct. At $l = 0{\cdot}63$ m, which corresponds to the *real* geometry of the rocket motor, the recorded sound pressure levels are of the same order as the ones found for the single restrictor case, implying that the restrictors "operate" virtually independently of each other. It must also be noted that, for $l = 0{\cdot}2$ m, a third, narrow and rather weak peak appears at relatively low velocities indicating that multiple resonant peaks with decreasing strength are possible when the flow velocity becomes smaller. A factor of approximately 3 separates the velocities corresponding to the first and third peaks.

Qualitatively similar observations can be made for the remaining two restrictor sizes. As shown in Figures 10(a) and 11(a), for fixed l, the velocity associated with resonant excitation increases with the restrictor internal diameter. For restrictor d_3 and $l \geq 0{\cdot}150$ m, [Figure 11(a)] the first, wide pass-band peak is no more visible, presumably because it is associated with velocity values larger than the experimental limit of 40 m/s. Indeed, for the case of $l = 0{\cdot}200$ m and assuming the same factor of 2 between the first and second peaks, it is found that the first resonant peak should occur at about 52 m/s. The same curve also shows a third small peak at 17 m/s, in agreement with the hypothesis that the velocities of the third and the first peak are related via a factor of 3.

The coupling between acoustic resonance and fluid flowfield can be seen in the cross-spectra of the hot wire and pressure transducer signals. These show clearly that the two signals are highly correlated and that the acoustic response is due to a *fluid dynamic perturbation.*

For conditions of maximum excitation, the amplitude of the pressure oscillations found is roughly 2·1 times the dynamic pressure of the mean flow. This amplitude is reduced to about 0·08 times the dynamic pressure in the single restrictor case. The corresponding values for velocity fluctuations vary between $0{\cdot}085U$ and $0{\cdot}025U$.

A global interpretation of the results should begin from the observation that the different curves shown in Figures 9(a), 10(a) and 11(a) present a striking similarity in shape and characteristics, with those found by Stoneman *et al.* (1988) for the case of resonant sound caused by flow past two plates placed in tandem in a rectangular duct. In this geometry, a vortex shedding frequency linearly dependent on the velocity was found to exist, accompanied by a very different type of behaviour in which resonant conditions were observed for some flow velocities. This resonance was attributed to the fact that acoustic perturbations feed back onto the shear layers separating from the trailing edge of the first plate and synchronize the frequency of the vortex shedding with one of the system acoustic modes. In

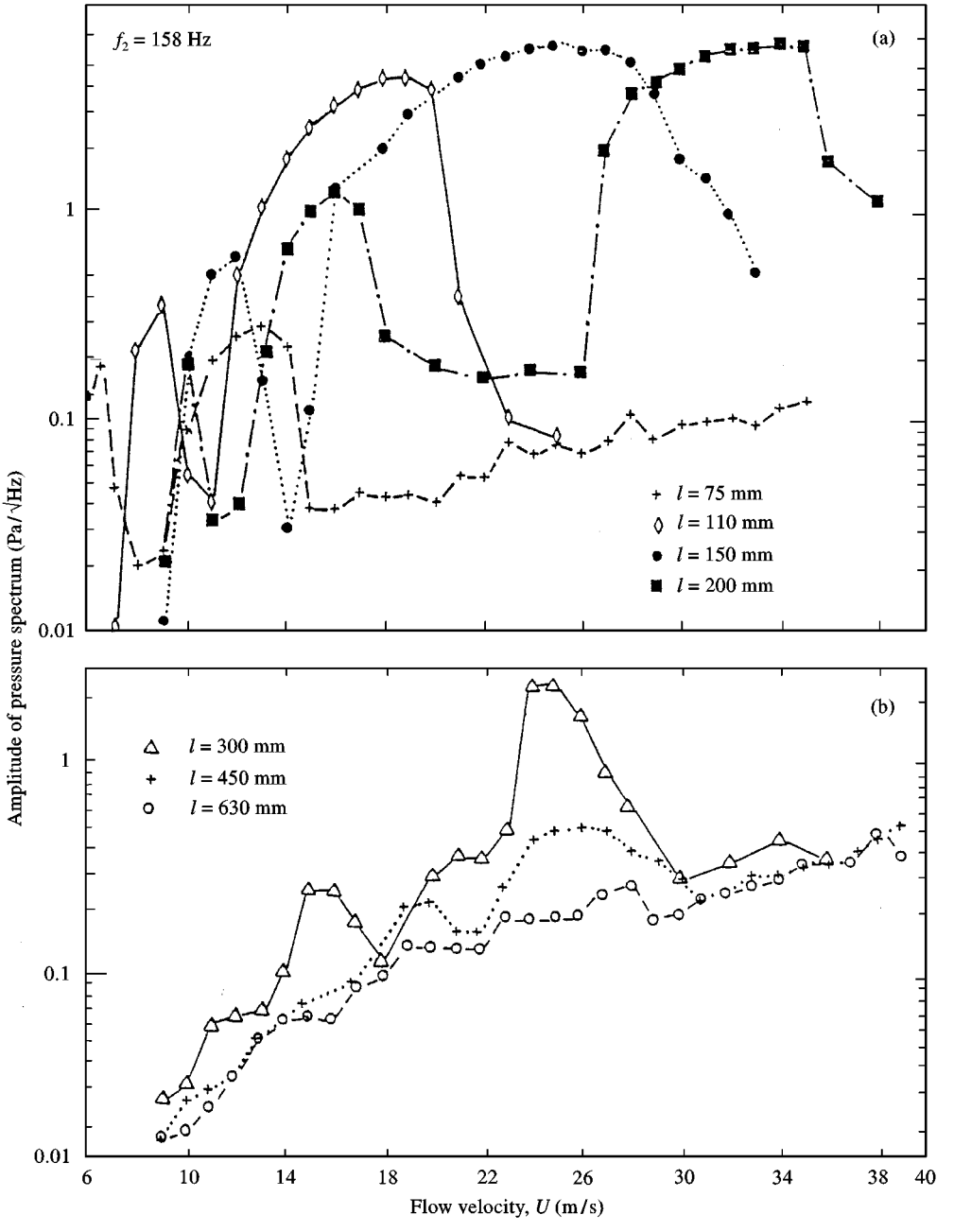

Figure 9. Amplitude of pressure spectrum at f_2 versus mean flow velocity for the d_1 restrictor pair (d_1 = 115 mm).

this case, the flow instability frequency remains locked-on to the acoustic frequency over a certain range of velocity values.

Re-examining the results of the present test campaign in the light of this similarity, evidence of vortex shedding outside the region of coupling with the acoustic modes was found for a few cases which are shown in Figure 12, where the frequency of velocity

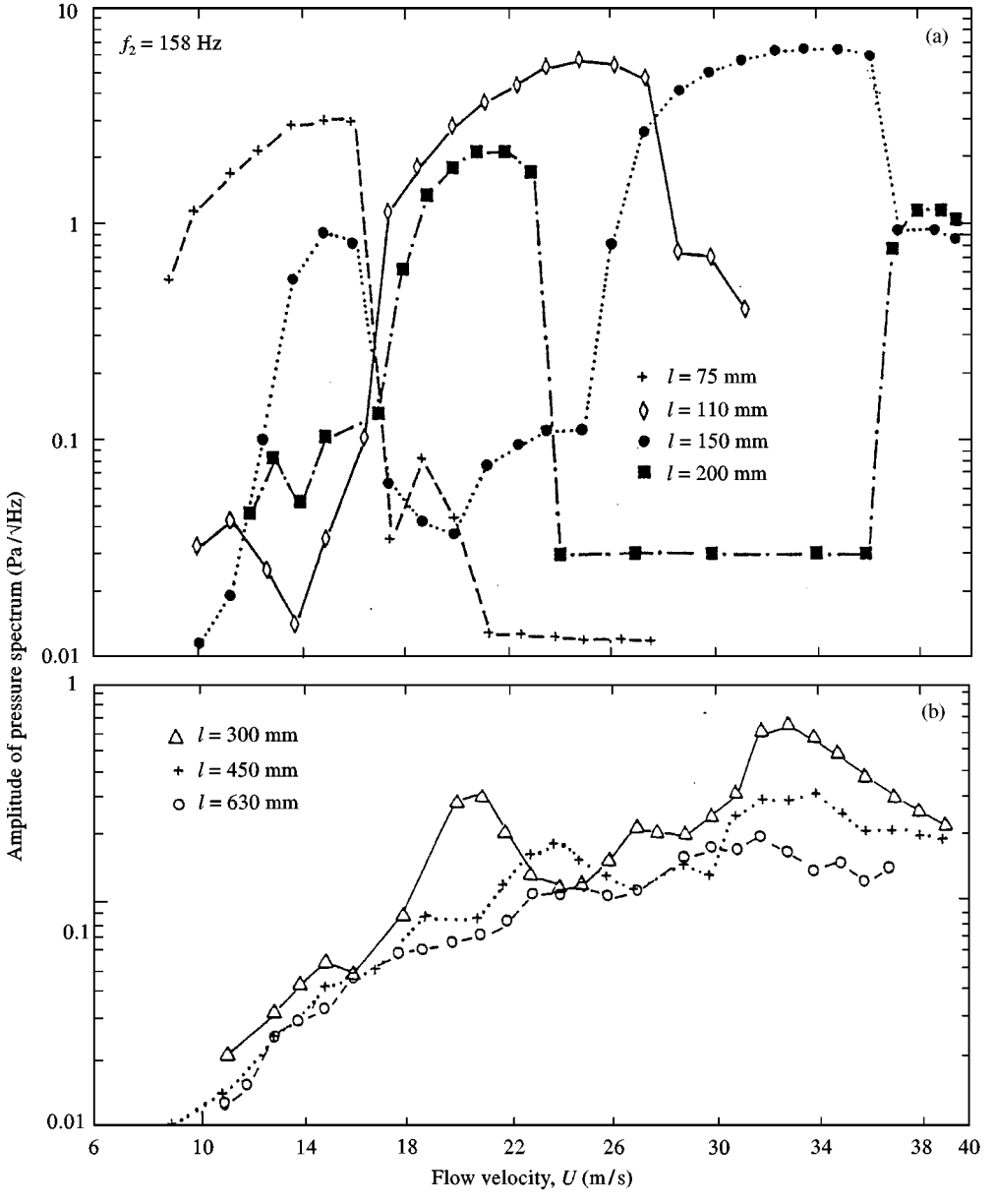

Figure 10. Amplitude of pressure spectrum at f_2 versus mean flow velocity for the d_2 restrictor pair ($d_2 = 125$ mm).

fluctuations is plotted versus flow velocity. The curves show lock-on to a fixed acoustic frequency for a range of velocities that coincides with the regions of resonant behaviour in Figures 9(a)–11(a). It can further be noticed that, the higher the sound pressure level at resonance, the wider is the lock-on velocity range.

On reaching the upper limit of the "resonant" velocity regime, the sound pressure level associated with the acoustic frequency is suddenly reduced, vortex shedding unlocks from the resonant sound field, while its frequency increases sharply towards the value corresponding to a constant Strouhal number behaviour and subsequently varies with velocity

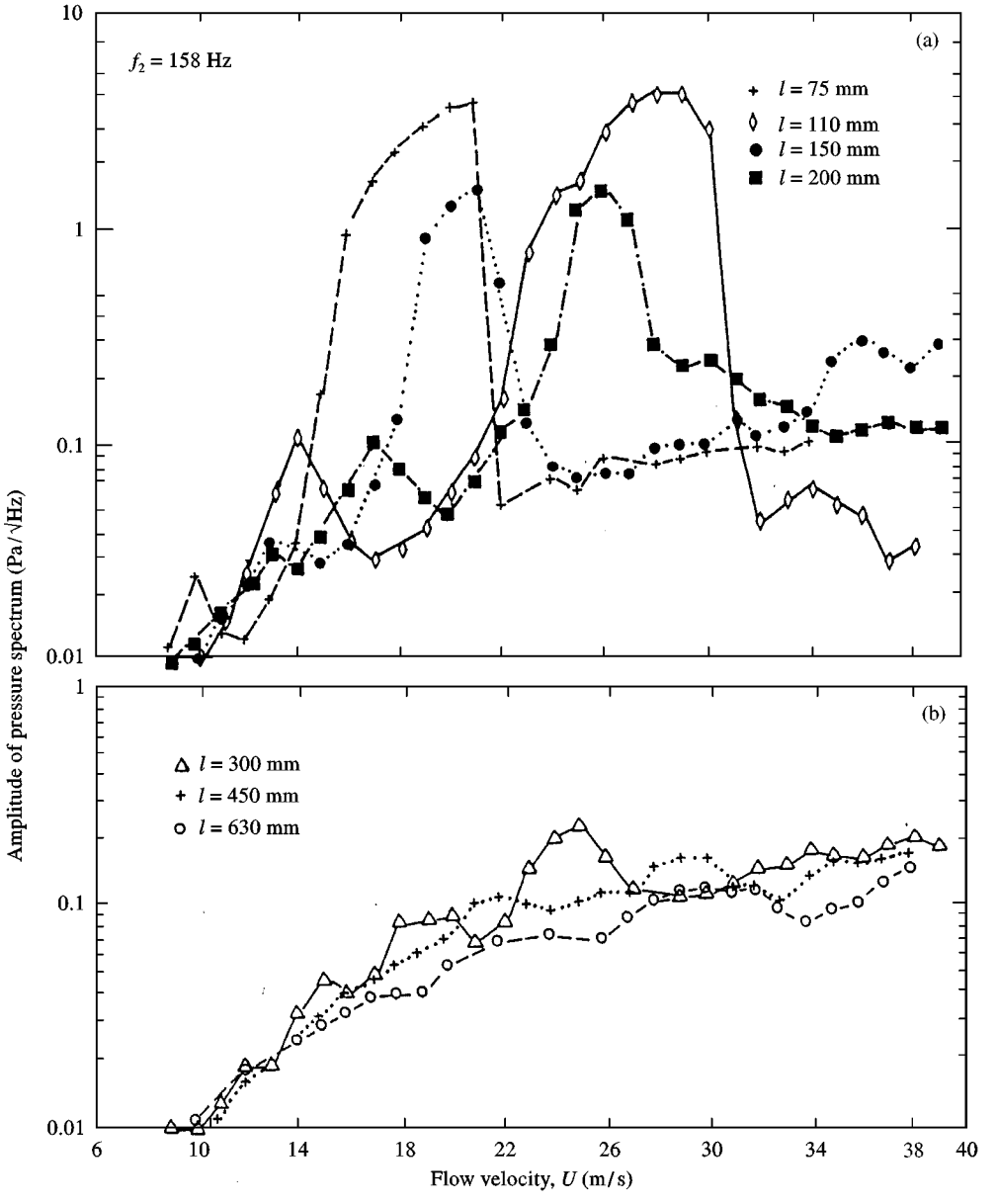

Figure 11. Amplitude of pressure spectrum at f_2 versus mean flow velocity for the d_3 restrictor pair ($d_3 = 134$ mm).

following a nearly linear law. For each restrictor size, a family of almost parallel straight lines is found, when the frequency f, which can be detected by both the pressure transducer and the hot wire, is sufficiently far from the acoustic modes f_2 and f_3.

From the slope of each of these families of curves, the Strouhal number for purely fluid-dynamic vortex shedding can be found for each restrictor diameter. These $S_D = f\,D/U$ values are approximately 0·5, 0·33 and 0·2 for d_1, d_2, and d_3, respectively.

From Figure 12 it can be seen that the data points for d_1 and $l = 0{\cdot}150$ m show how vortex shedding firstly unlocks from the resonant sound field for $U > 11$ m/s and reaches

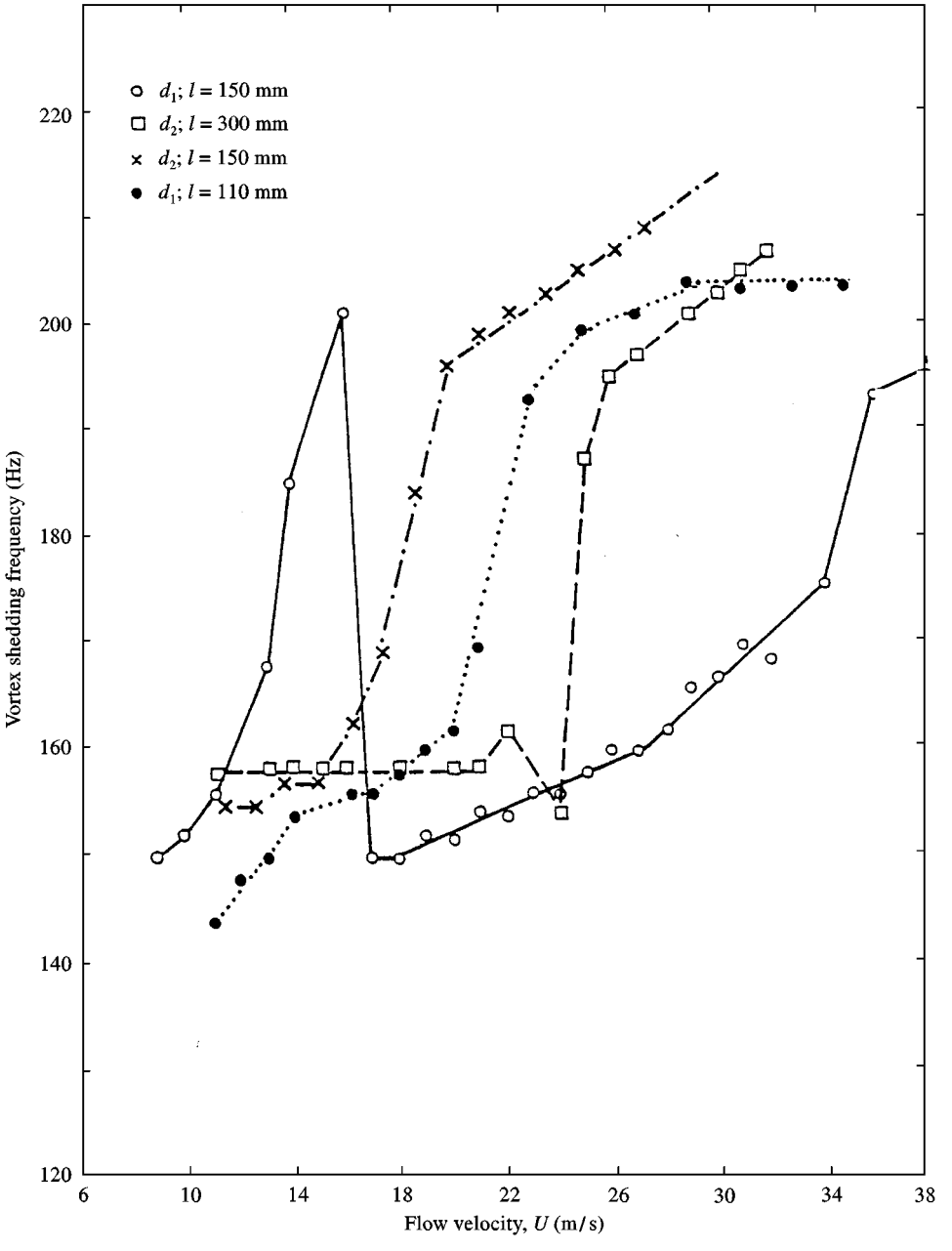

Figure 12. Fluid dynamic vortex shedding and "lock-on" phenomenon.

the Strouhal number corresponding to fully fluid-dynamic behaviour, then locks again on the same acoustic mode (at $U = 17$ m/s) for a wide velocity band. For the same d and $l = 0{\cdot}110$ m, vortex shedding remains locked onto f_2 for flow velocities between 13 and 18 m/s. It briefly unlocks as velocity increases but, before complete recovery of natural behaviour, it locks again onto the harmonic f_3. Apart from the data points in Figure 12, all other cases tested did not produce a repeatable vortex-shedding signal outside the resonant ranges.

4. A MODEL FOR THE BEHAVIOUR OF THE SYSTEM

It clearly emerges from the afore-discussed experimental results that the three different restrictors tested seem to fit in a unique pattern of behaviour, thus justifying an attempt to put in evidence and model the basic mechanism underlying the interaction between fluid dynamic and acoustic instabilities in the present system.

In this perspective, the first conclusion to be drawn is that the present results are in broad agreement with Huang & Weaver (1991) and especially with the already quoted findings of Hourigan *et al.* (1990). The latter is true particularly for values of l such that strong interaction between restrictors exists. Indeed, for those l-values resonant sound generation at the frequency of an acoustic mode is found for different velocity ranges, which could well correspond to the existence of one, two, three and so on vortices between the restrictors. This hypothesis is supported by the fact that a linear 1, 2, 3, … relationship exists between the different critical velocities. Moreover, the observation that, for the same value of l and the same harmonic, the corresponding critical velocity values increase with decreasing restrictor height agrees well with this interpretation. It can then be tentatively concluded that resonant conditions are achieved when the vortices shed by the upstream obstacle impact on the downstream one with a phase offset to the acoustic cycle such that a net increase of acoustic energy is produced.

With respect to Hourigan *et al.* (1990), the present data put in evidence the fundamental role of the parameter l: it is clear that a transitional distance l_t exists above which mutual interaction between restrictors becomes so weak that they can be considered independent of each other, and that l_t increases with restrictor height. The same trend can be observed for the distance l_m at which maximum interaction and therefore highest resonant sound level occurs.

These observations, together with simple physical considerations, lead us to propose a model of restrictor behaviour based upon the nature of the flowfield behind it. On the restrictor, flow separation occurs and a recirculating region is formed behind it, followed by a highly perturbed reattaching layer where the flow gradually recovers its state of equilibrium. It is postulated that significant interaction between the two obstacles can exist only if the flow reaching the downstream one has not recovered fully its equilibrium condition. For the case of developed turbulent flow, the typical length of the separated region behind a very thin obstacle is 8–12 times its height h, while recovery may well require an additional length of 10–15h (Bullock *et al.* 1990; Schofield & Logan 1990; Liou *et al.* 1990). These lengths can be compared to the experimental bounds obtained for l_t/h and l_m/h and shown in Table 1.

It is clear that, for the values of d/D tested, the strongest resonance is reached when the distance between the restrictors is of the order of the separated region behind an isolated obstacle, in other words, when l falls in a region of high turbulence. Mutual interaction practically ceases when the flow impinging on the second restrictor has fully recovered the equilibrium condition.

TABLE 1
Distances between restrictors above which mutual interaction ceases (l_t/h) and at which maximum interaction is observed (l_m/h)

h (m)	d (m)	l_t/h	l_m/h
0·0175	0·115	26–34	9·0–11·0
0·0128	0·125	25–35	8·5–12·0
0·0080	0·134	30	9·5–14·0

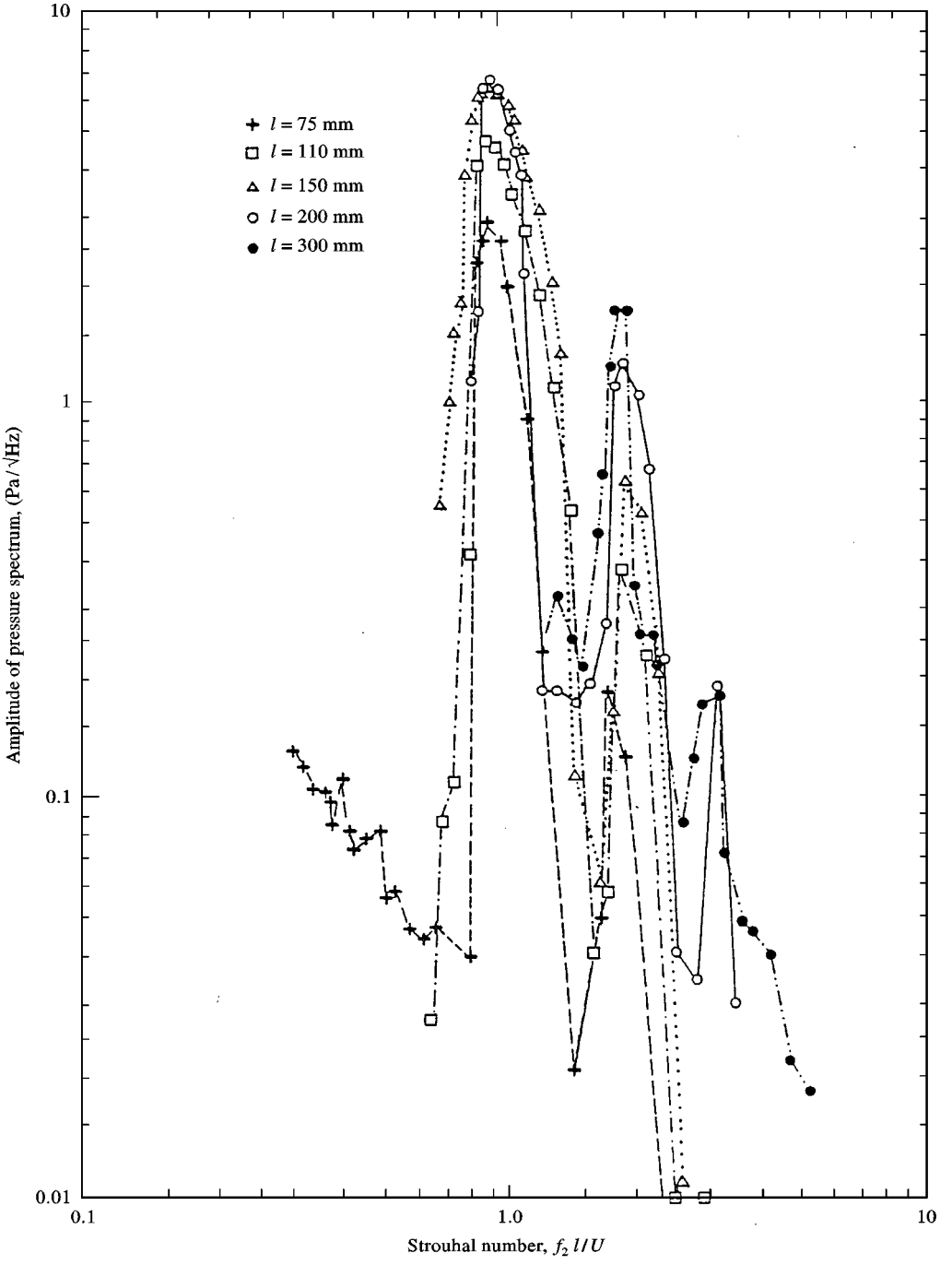

Figure 13. Critical Strouhal number for pair of d_1 restrictors.

A unified approach to a quantitative description of the phenomenon may be based on the "acoustic" Strouhal number defined in equation (1). If the data presented in Figures 9–11 are replotted in terms of energy level versus S (Figures 13–15), it is observed that the

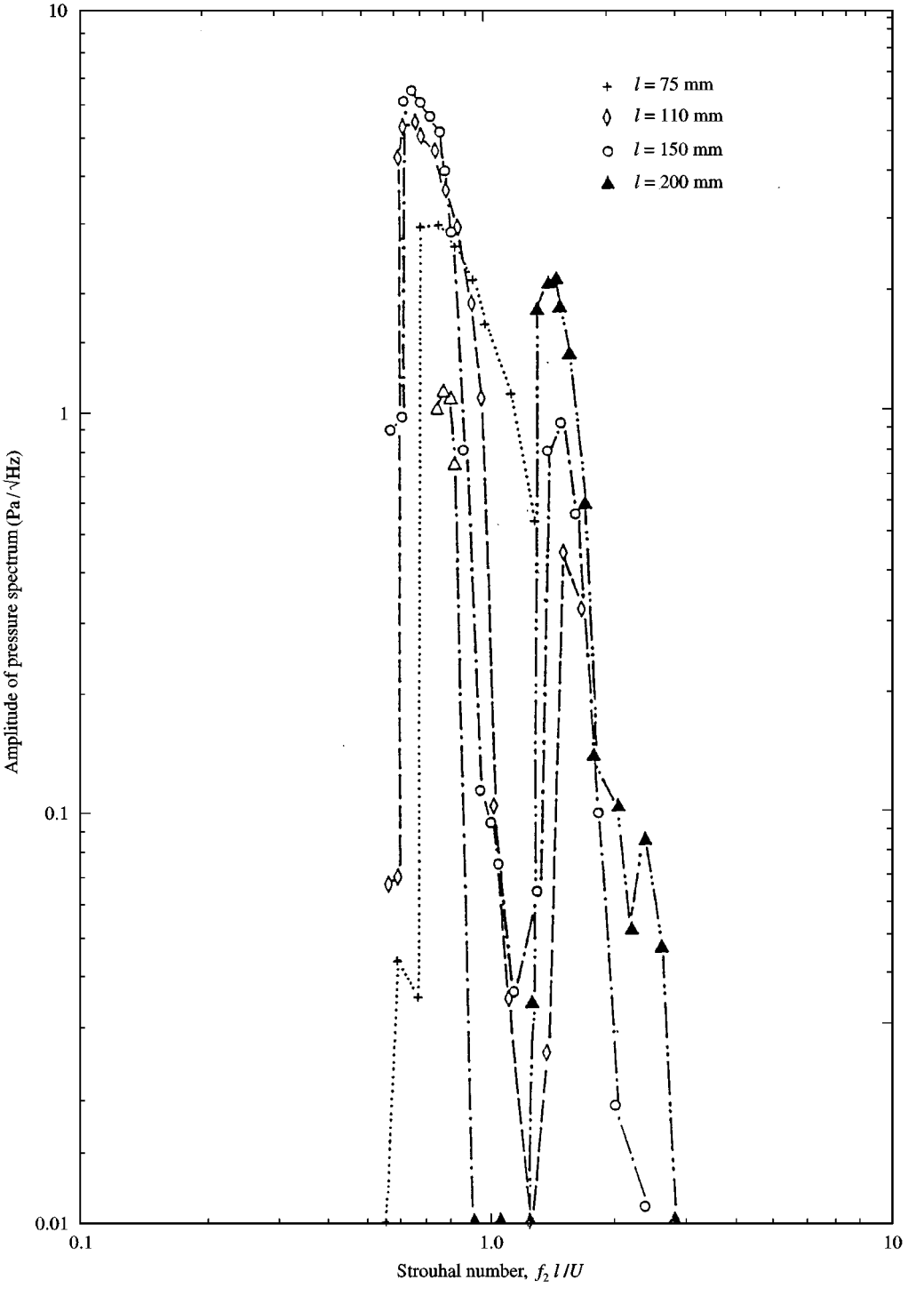

Figure 14. Critical Strouhal number for pair of d_2 restrictors.

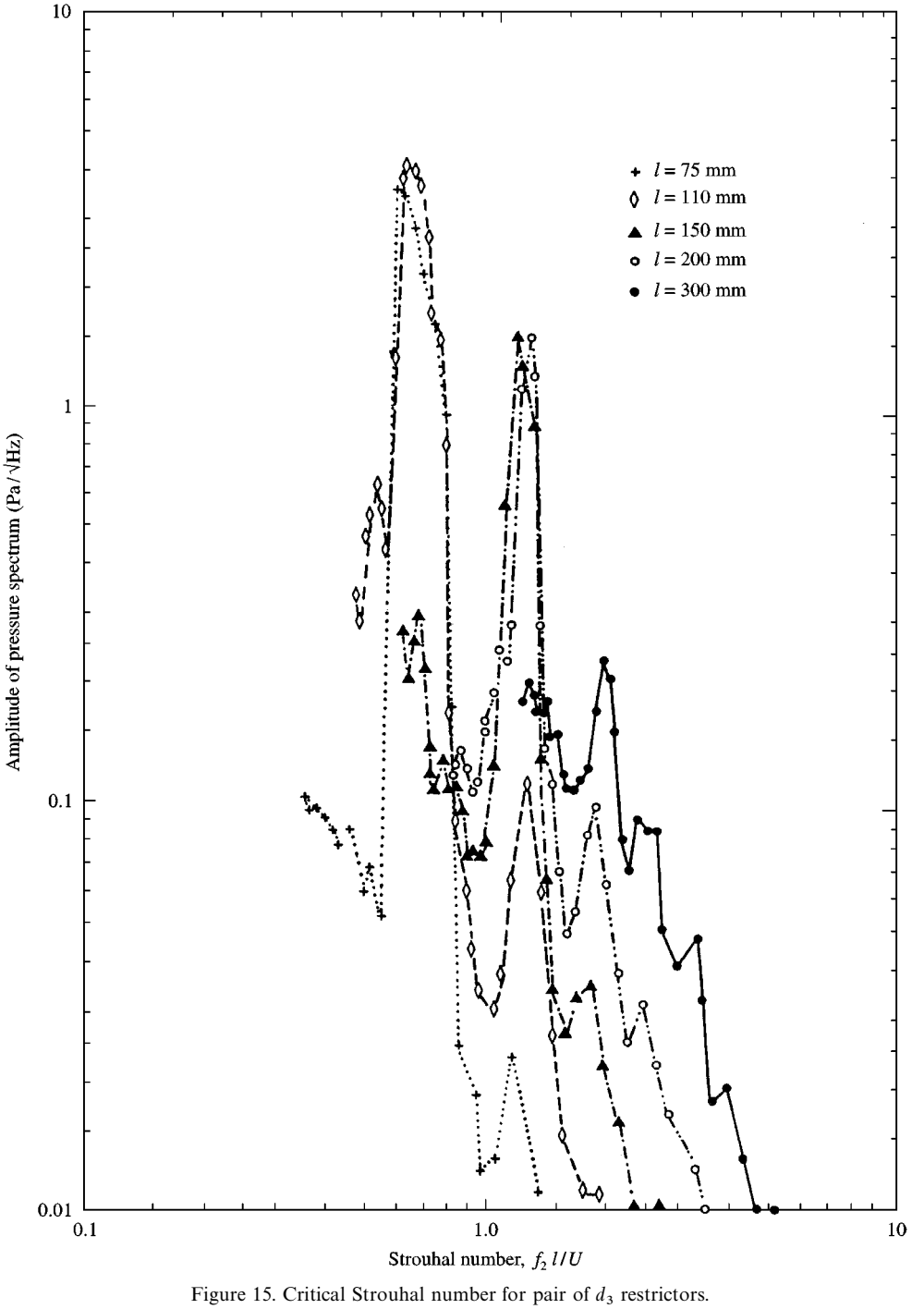

Figure 15. Critical Strouhal number for pair of d_3 restrictors.

excitation peaks for all curves are associated with almost the same Strouhal numbers, which are summarized in Table 2.

As expected, S_2, S_3, etc. result from S_1 after multiplying by 2, 3, … respectively, and are taken to correspond to the resonant conditions with a number of vortices between obstacles

TABLE 2
Strouhal numbers corresponding to peaks in Figures 9–11

d (m)	S_1	S_2	S_3	S_4
0·115	0·9–0·95	1·75–1·95	2·6–2·7	3·3–3·6
0·125	0·7–0·75	1·40–1·60	2·1–2·25	3·0–3·1
0·134	0·56–0·66	1·15–1·25	1·8–1·9	2·3–2·4

equal to the subscript of S. For each l, a flow velocity $U_1 = f_2 l/S_1$ exists corresponding to maximum resonant energy, while $U_1/2$, $U_1/3$, … also produce resonant oscillations of decreasing intensity; as expected, S_1 increases with restrictor height.

Figure 16 exemplifies how the main parameters affecting resonant sound generation (l, U, d, D, f_2) can be correlated by a simple relation, taking the form

$$S_n = \frac{f_2 l}{U_n} = nC\left(\frac{d}{D}\right)^a, \tag{2}$$

where $a = 1$, $n = 1, 2, \ldots$, and C is a coefficient, constant for each value of d, which takes the value 1·2 for d_1, 0·9 for d_2 and 0·65 for d_3. The straight lines in Figure 16 represent relation (2) for $n = 1$, 2 and 3 (similar fits are obtained for all restrictor sizes tested). It has to be noted that such a simple relationship is *predictive* insofar as it provides $S_1, S_2, S_3, \ldots$, values associated with the excitation peaks once C is known.

A better insight on the role and value of C can be attained keeping in mind that the main effect of a change in restrictor size is upon the speed of travel of vortical disturbances in the flow. This speed can be roughly approximated by taking it equal to 60% of the flow velocity at the restriction (Jou & Menon 1990; Flatau & Van Moorhem 1990). For two resonant situations characterized by one vortex between the obstacles, identical l values and different restrictor sizes, the frequency of arrival of vortices at the downstream restrictors should be the same (so that vortex passage happens at the same phase of the acoustic cycle). This means that the speed of disturbances in the flow is the same in both configurations:

$$0{\cdot}6\ U_1\left(\frac{D}{d}\right)^2 = 0{\cdot}6\ U_1'\left(\frac{D}{d'}\right)^2$$

or

$$\frac{U_1}{U_1'} = \left(\frac{d}{d'}\right)^2 \tag{3a}$$

which, taking equation (2) into account, gives

$$\frac{S_1}{S_1'} = \frac{C}{C'}\frac{d}{d'} = \frac{U_1'}{U_1}$$

or

$$\frac{C}{C'} = \frac{U_1'}{U_1}\frac{d'}{d} = \left(\frac{d'}{d}\right)^3. \tag{3b}$$

The values of C found empirically agree well with equation (3b) lending support to the proposed approach. In addition, relation (3b) offers a way to predict the critical values of S and therefore the conditions of resonance for any restrictor size once a single d/D value has been tested. Assuming that the model and the correlation remain valid for values of d/D very close to unity, the value of S_1 for $d/D \approx 1$ obtained from equations (2) and (3b) is 0·56,

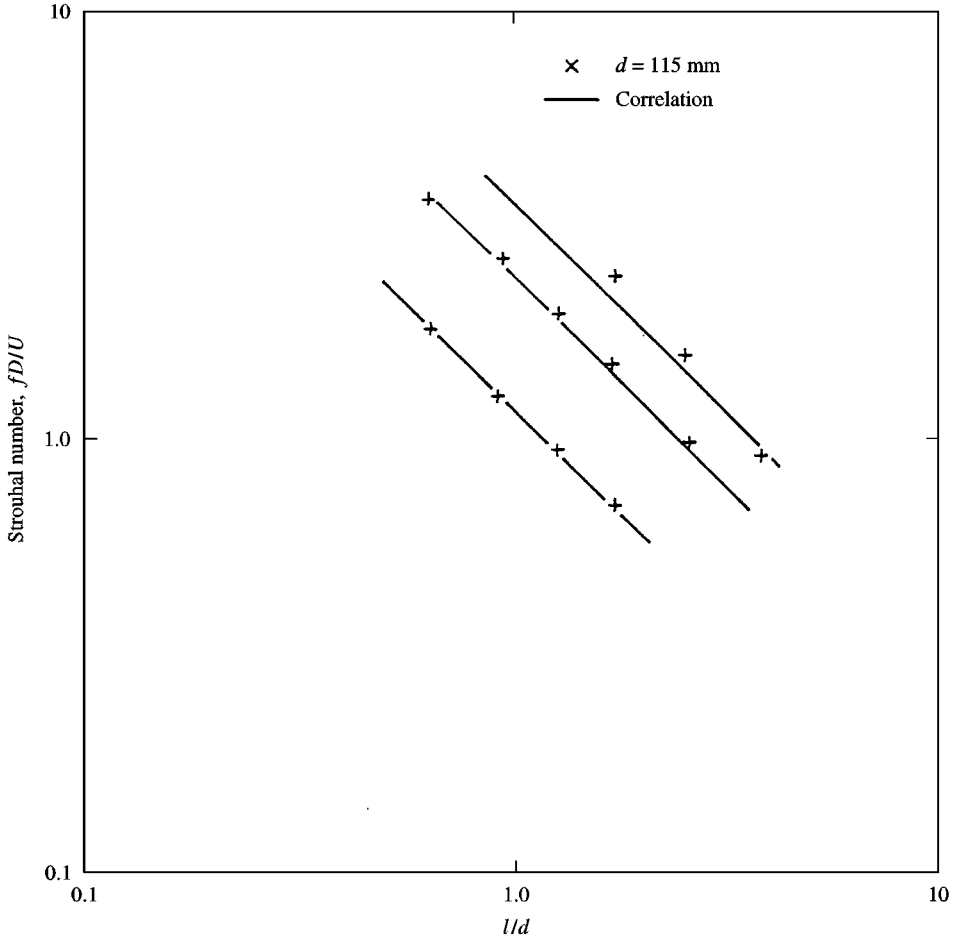

Figure 16. Plot of f_2D/U versus l/d. Pair of d_1 restrictors. The lines correspond to different number of vortices between the restrictors.

close to the one found for instability phenomena in pipes without restrictors. The interesting implication arising is that if this value is universal, then the correlations developed herein constitute a prediction method for the resonant regimes in any tube and for restrictor sizes $0{\cdot}7 < d/D < 1$. The validity of this statement remains to be confirmed by tests with varying tube diameters.

In the framework of the present model, an interpretation of the observations made for the single restrictor case is also possible. The excitation peaks exhibited by the curves for the two smaller restrictor heights in Figure 8 correspond to 'acoustic' Strouhal numbers that fit closely the S_3, S_4 values for d_2 and the S_4, S_5, S_6 values for d_3 if the distance between restrictor and nozzle ($\approx 0{\cdot}6$ m) is used for the calculation. This means that the slight enhancement of sound level, found for some values of flow velocity, is caused by the interaction between the single obstacle and the downstream nozzle and characterized by the presence of an integer number of vortices in this region. Although the distance of 0·6 m should be, according to the mechanism proposed, large enough to ensure no interaction, hot-wire measurements of radial velocity show that, in the specific geometry examined here, the flow reaching the nozzle has not fully recovered yet and is indeed characterized by high turbulence intensity. The main reason for such extended separation and recovery lengths behind the restrictor is the presence of the small cavity just ahead of the obstacle.

5. DISCUSSION-METHODS TO CONTROL RESONANCE

The previous discussion has shown that the present experimental results are in general agreement with the conclusions of Hourigan *et al.* (1990); however, it should be mentioned that these authors performed tests using much lower flow velocities (0–5 m/s) than those for which strong resonance has been found in the present test-section. The reason why the two expreriments can be compared lies in the already reported trend of increasing S_1 (decreasing U_1) with increasing restrictor height. Hourigan *et al.* (1990) used a rectangular test-section with a ratio between restriction and duct size of 0·37, considerably smaller than the present d/D values; the corresponding value of S_1 was found to be 4·7. Introducing $d = 0{\cdot}37D$ in equation (3b) a value of approximately 4·0 is obtained for S_1, reasonably close to the experimental one. It must be kept in mind that the rectangular duct was completely open at its end and did not allow for any interaction between obstacles and outlet.

This is not the case for the test section used by Flatau & Van Moorhem (1990), where significant interaction between restrictor and nozzle was found. Such interaction manifests itself with the presence of fluctuations at the frequencies of the acoustic modes corresponding to wavelengths equal to the distances between each obstacle and the tube end. In other words, the observed frequencies vary with the position of the restrictors in the tube. This behaviour could be attributed to the fact that the height of the restrictors is quite important when compared to the tube diameter (58 mm versus 114 mm), while distances between obstacle and nozzle are less than 30 restrictor heights. In view of the disagreement between available evidence, two additional experiments were performed in the present test-section. Firstly, a pair of restrictors of diameter d_1 was installed with the upstream obstacle located at $L/2$ and the downstream one at different positions between the first and the nozzle, to excite any possible mode due to downstream restrictor–nozzle interaction at a frequency other than the tube acoustic modes. The results found are, as anticipated, quite similar to the ones described previously with the upstream restrictor in the first half of the tube. Critical frequencies and characteristic Strouhal numbers $S_1, S_2, \ldots$, show no difference with respect to the results previously described, supporting the model of behaviour proposed above. The only noticeable change observed is a slight decrease of the sound pressure levels at resonant conditions. The reason is most probably the fact that now the pressure node for f_2 lies close to the upstream restrictor rather than the downstream one. This last condition has already been qualified as less favourable for strong resonance.

The second series of tests involves the use of restrictors with a d value of 0·07 m, i.e., a d/D ratio considerably lower than before and similar to the value used by Flatau & Van Moorhem (1990). In this case it is found that, apart from the expected modes at frequencies related to the total length of the tube, new frequencies with comparable levels of energy content appear,which can be associated with a 'tube' of length equal to the upstream restrictor–nozzle distance. Additionally, it should be noted that vortex shedding in the form of a peak whose frequency varies linearly with the velocity is stronger and easier to detect. It can be concluded that the system behaves in agreement with the model described in the previous sections for rather small obstacles with values of d/D in the range 0·7–1·0. For larger restrictor sizes, characterized by a d/D ratio of the order of 0·5 or less, more acoustic frequencies interfere and the overall picture becomes more complicated, as reported by Flatau & Van Moorhem (1990).

Finally, some efforts were made in order to achieve reduction of the amplitude of the resonant sound pressure oscillations. The injection of side flow through the cavity upstream of the $L/2$ restrictor (see Figures 1 and 2) was expected to affect the behaviour of the shear

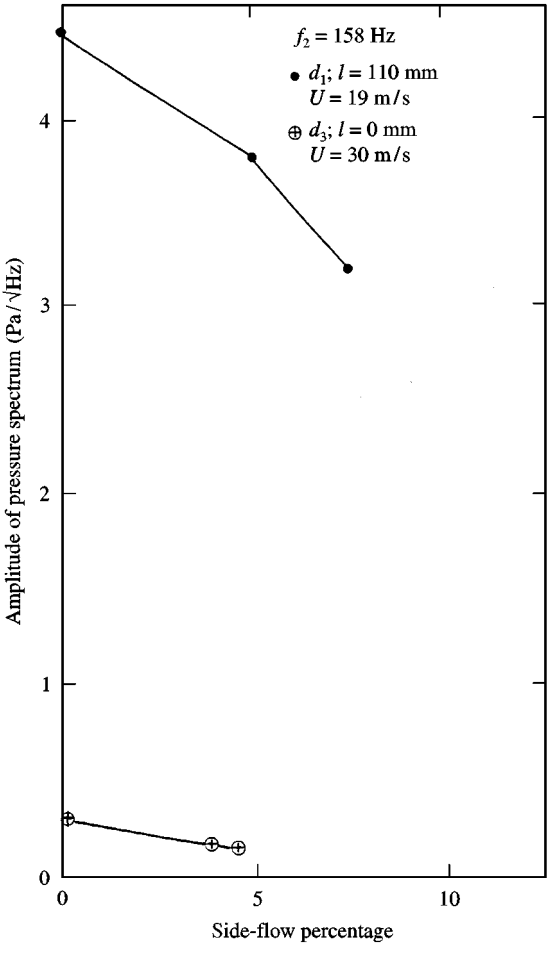

Figure 17. Effect of side flow injection on the pressure spectrum amplitude.

layer impinging on it and thus disturb the mechanism responsible for resonance. In fact, by injecting a side-flow corresponding to 7% of the total longitudinal flowrate, a 30% reduction of the fluctuation amplitude at resonant conditions is obtained, as shown in Figure 17.

Given the dependence of S_1 on the d/D value, some tests were also run to investigate the effect of a restrictor with non-circular, irregular edge. The results present no difference at all with respect to the normal geometry with a smooth circular edge.

Circumferential pressure measurements at two different cross-sections, one in each half-segment of the test-section, have proved that the oscillations at frequency f_2 take place without any appreciable circumferential phase difference. A phase difference of π was found between the two tube segments, in agreement with the fact that the location of pressure node for the standing wave at f_2 is very close to the $L/2$ location. On the basis of these observations, it was decided to cut the movable upstream ring into two semicircular pieces and place them in a way such that each piece lies at a different distance from the downstream restrictor (Figure 18). A separation of only 3 mm between the two half-restrictors proved enough to reduce by almost 60% the sound level at resonance. For distances between the two semicircular elements larger than 10 mm, resonance is

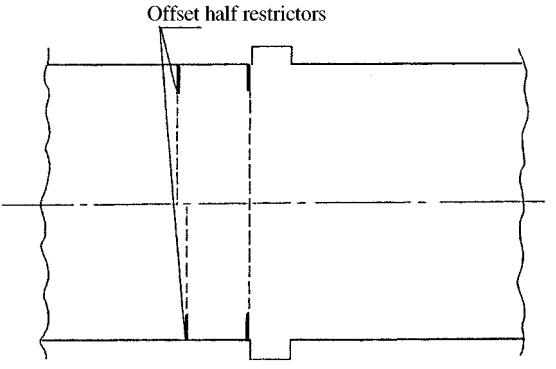

Figure 18. Damping of fluid-dynamic-acoustic instability: one restrictor replaced by two semicircular pieces a few mm apart.

completely eliminated and the energy levels reach the magnitude of those found for the single restrictor case. This result is a straightforward consequence of the circumferential phase uniformity mentioned above and agrees well with the mechanism of instability proposed herein, which requires a specific space–time distribution of flow instabilities between the two obstacles for self-sustained resonance to occur. The arrival of vortices at the second obstacle at a fixed phase with respect to the acoustic cycle is not possible in this configuration and self-sustained resonance becomes progressively more difficult to achieve as the two pieces are placed further apart from each other. This important result implies that similar reduction of the oscillation amplitude should be obtained by simply placing the upstream restrictor slightly inclined in the tube, a suggestion that may prove useful for the design of solid fuel boosters.

6. CONCLUSIONS

The problem of aerodynamically generated acoustic resonance was experimentally investigated in a tube containing a single or a pair of annular flow restrictors. It is found that strong resonance occurs at several flow velocities corresponding to the existence of one, two or more vortices between the obstacles. This is valid as long as the distance l between restrictors is not larger than the length of the flow recovery region behind the upstream ring. Actually, maximum sound levels are observed when l is of the order of 10–12 obstacle heights, i.e., when the downstream restrictor lies in the highly perturbed flow regime around the reattachment point for the separated flow behind the first restrictor. For $l > 25$–$30h$, i.e., when the impinging flow has fully recovered its equilibrium state, the two restrictors behave independently. The different cases examined are shown to follow a unique pattern when nondimensionalized in terms of the "acoustic" Strouhal number. The values of S associated with each resonant region, $S_1, S_2, \ldots$, are found to correlate linearly with d/D. Simple physical arguments based on an estimation of the vortical speed of travel, allow for a meaningful interpretation of the empirical coefficients involved in the correlation proposed. Some evidence concerning locking of the vortex-shedding frequency by the second acoustic mode is also reported. Possibilities of reducing the resonant sound levels via side-flow injection, but mainly by splitting the first ring into two semicircular pieces and setting an offset distance between them, are discussed. This latter finding suggests that use of a restrictor with a slight inclination in real rocket combustion chambers might help eliminating undesired resonant oscillations.

ACKNOWLEDGEMENTS

The present study has been supported financially by BPD (Italy) in the framework of the combustion stability assessment of the Ariane 5 booster.

References

Anthoine, J., Planquart, P. & Olivari, D. 1998a Cold flow investigation of the flow acoustic coupling in solid propellant boosters. AIAA Paper 98-0475.

Anthoine, J., Olivari, D., Hulshoff, S. & Van Rooij, M. 1998b Qualitative model of vortex induced oscillations in a model of solid propellant boosters. AIAA Paper 98-2270.

Brown, R. S., Dunlap, R., Young, S. W. & Waugh, B. G. 1981 Vortex shedding as a source of acoustic energy in segmented solid rockets. *Journal of Spacecraft and Rockets* **18,** 312–319.

Bruggeman, J. C., Hirschberg, A., Van Dongen, M. E. H. & Wijnands, A. P. J. 1991 Self-sustained aero-acoustic pulsations in gas transport systems: experimental study of the influence of closed side branches. *Journal of Sound and Vibration* **150,** 371–394.

Bullock, K. J., Lai, J. C. S. & Walker, T. B. 1990 Flow measurements behind attached ring-type turbulence promoters. *Physics of Fluids* A **2,** 390–399.

Dunlap, R. & Brown, R. S. 1981 Exploratory experiments on acoustic oscillations driven by periodic vortex shedding. *AIAA Journal* **19,** 408–409.

Flandro, G. A. 1986 Vortex driving mechanism in oscillatory flows. *Journal of Propulsion and Power* **2,** 206–214.

Flatau, A. & Van Moorhem, W. 1990 Prediction of vortex shedding responses in segmented solid rocket motors. *AIAA Paper* 90–2073.

Hegde, U. C. & Strahle, W. C. 1985 Sound generation by turbulence in simulated rocket cavities. *AIAA Journal* **23,** 71–77.

Hourigan, K., Welsh, M. C., Thompson, M. C. & Stokes, A. N. 1990 Aerodynamic sources of acoustic resonance in a duct with baffles. J*ournal of Fluids and Structures* **4,** 345–370.

Huang & Weaver 1991 On the active control of shear layer oscillations across a cavity in the presence of pipeline acoustic resonance. *Journal of Fluids and Structures* **5,** 207–219.

Jou, W. H. & Menon, S. 1990 Modes of oscillation in a nonreacting ramjet combustor flow. *Journal of Propulsion and Power* **6,** 535–543.

Kriesels, P. C., Peters, M. C. A., Hirschberg, A., Wijnands, A. P. J., Iafrati, A., Riccardi, G., Piva, R. & Bruggeman, J. C. 1995 High amplitude vortex induced pulsations in gas transport systems. *Journal of Sound and Vibration* **184,** 343–368.

Liou, T. M., Chang, Y. & Hwang, D. W. 1990 Experimental and computational study of turbulent flows in a channel with two pairs of turbulence promoters in tandem. *ASME Journal of Fluids Engineering* **112,** 302–310.

Menon, S. & Jou, W. H. 1990 Numerical simulations of oscillatory cold flows in an axisymmetric ramjet combustor. *Journal of Propulsion and Power* **6,** 525–534.

Michalke, A. 1972 The instability of free shear layers: a survey on the state of the art. *Progress in Aerospace Sciences* **12,** 213–239.

Nomoto, H. & Culick, E. C. 1982 An experimental investigation of pure tone generation by vortex shedding in a duct. *Journal of Sound and Vibration* **84,** 247–252.

Rockwell, D. & Naudascher, E. 1978 Self-sustaining oscillations of flow past cavities. *ASME Journal of Fluids Engineering* **100,** 152–165.

Schofield, W. H & Logan, E. 1990 Turbulent shear flow over surface mounted obstacles. *ASME Journal of Fluids Engineering* **112,** 376–385.

Stoneman, S. A. T., Hourigan, K., Stokes, A. N. & Welsh, M. C. 1988 Resonant sound caused by flow past two plates in tandem in a duct. *Journal of Fluid Mechanics* **192,** 455–484.

Tritton, 1988 *Physical Fluid Dynamics*. Oxford: Oxford University Press.

APPENDIX: NOMENCLATURE

C	semi-empirical constant
c	speed of sound
D	tube diameter

d	restrictor opening
d_n	nozzle diameter
f	frequency
h	height of the obstacle (restrictor)
L	tube length
l	distance between restrictors
l_t	distance between restrictors above which mutual interaction ceases
l_m	distance between restrictors at which maximum interaction occurs
Re	Reynolds number
S	Strouhal number
U	mean flow velocity